Current Topics in Biophysics 2002, 26(1), 7-14

AQUEOUS SAMPLE CONSIDERATIONS IN UNIFORM FIELD RESONATORS FOR ELECTRON PARAMAGNETIC RESONANCE SPECTROSCOPY

JAMES S. HYDE[1], RICHARD R. METT[1,2]

[1]Biophysics Research Institute, Medical College of Wisconsin, Milwaukee, Wisconsin USA 53226-0509;
[2]Milwaukee School of Engineering, Milwaukee, Wisconsin USA 53202-3109.

A new class of cavity resonators for use in EPR spectroscopy has recently been introduced by Mett, Froncisz and Hyde (*Rev. Sci. Instrum*. 72, 4188, 2001) that oscillate in what were termed "uniform field" modes. In these cavities, the RF magnetic field is uniform along an axial sample tube. The present paper is a theoretical analysis of flat aqueous sample cells in the uniform field resonator designated TE_{U02}, which is an analogue of the widely used rectangular TE_{102} cavity. A full wave solution in the presence of sample loss was found. Samples that saturate with the available RF magnetic field and those that do not are considered. A geometry is described that requires four times more sample than in a conventional cavity, and yields three times higher EPR signal intensities for saturable samples such as spin labels. It was concluded that not only is the quality of the EPR data improved in these resonators because the RF field is uniform over the sample, but also the signal-to-noise ratio can be better.

INTRODUCTION

Axially uniform resonant cavity modes for use in electron paramagnetic resonance (EPR) spectroscopy were recently introduced from this laboratory (Mett, Froncisz & Hyde, 2001). The commonly used cylindrical transverse electric TE_{011} and rectangular TE_{102} modes were considered. In the cylindrical and rectangular mode geometries, the sample is along the axis of the cylinder, dielectric disks of 1/4 wavelength thickness are placed at each end wall, and the diameter of the cylinder is set at the cutoff condition for microwave propagation in cylindrical waveguide at the desired microwave frequency. It was shown theoretically and experimentally that the microwave magnetic field, and therefore the curl of the electric field, is uniform along the sample in the region between the disks and that the resonant frequency is independent of the length of the cylinder. Uniformity of the microwave field over the sample is highly desirable in EPR spectroscopy. The rectangular TE_{102} geometry is analogous, noting that the microwave field is uniform in a plane. The new microwave modes for the cylindrical and rectangular geometries were designated TE_{01U} and TE_{U02}, where U stands for "uniform."

The present paper is concerned with aqueous EPR sample geometries in axially uniform rectangular geometries. We consider flat-cell samples of various cross sections extending the length of the resonator. It is a theoretical paper employing analytical solutions of electromagnetic field distributions at X-band (9.5 GHz), extending the work of Mett *et al.* (2001) to the flat-cell geometry.

The earliest discussion of aqueous sample-cell geometries seems to be that of Hirshon and Fraenkel (1955). Stoodley (1963) wrote a seminal paper on the subject following the treatment of EPR sensitivity of Feher (1956). Stoodley considered full-wave solutions of fields in the presence of sample in the limit of lossless sample [$\mathrm{Im}(\varepsilon_s) = 0$] and compared the results to the unperturbed field or "empty cavity" limit, also subsequently discussed by Wilmshurst (1967). Stoodley found that differences in predictions of these two limits were small – on the order of several percent. Our work extends these results to include the full wave solution in the presence of sample loss and compares the TE_{102} mode to the TE_{U02} uniform field mode.

In retrospect, Stoodley's paper was flawed by failing to recognize that differing sample cell geometries are required depending on whether or not the EPR signal can be saturated with the available microwave power. Hyde (1965) introduced a general system of sample classification, asking three questions: does the EPR signal exhibit microwave power saturation at the available incident power, is it limited in size or volume, and does it exhibit dielectric loss? He suggested that EPR sensitivity analysis ought to be carried out for each of the resulting eight classes of samples. Wilmshurst (1967) used this framework in his analysis of aqueous sample cell geometries. Wilmshurst's

results for saturable and non-saturable unlimited aqueous samples are summarized in Table l. The "saturable sample" case implies that the incident power is readjusted to hold H_1 at the sample constant. The non-saturable case implies that the incident microwave power is constant. The early literature on this subject is extensive. Poole (1983) provides access to these papers and Alger (1968) gives additional background. Following Table 1, the present paper provides comparable information for uniform field rectangular modes and gives sensitivities for uniform field modes compared with conventional modes.

An additional complication occurs when analyzing microwave characteristics of uniform field resonators containing aqueous samples. Mett *et al.* (2001) showed that when a sample is inserted, the uniformity of the field is degraded. The uniformity can, in principle, be recovered in one of two ways: (i) at constant microwave frequency the resonator radius can be made smaller; (ii) at constant resonator radius, the dielectric thickness can be made thicker, resulting in a uniform field at a lower microwave frequency.

Neither alternative is practical for general-purpose usage. The perturbations caused by the sample will generally be small; nevertheless, the resulting inhomogeneity of the field over the sample is of interest to the investigator. Inhomogeneities for optimum sample sizes were calculated here. The axial field nonuniformities resulting from sample insertion considered here were found to be on the order of < 0.1%.

A major advantage of uniform field modes is that the electric field distribution across the sample is uniform along the axis of the sample. For conventional cavities, the curl of the electric field varies along the sample axis sinusoidally. In principle, it would be appropriate to design a sample cell geometry with optimized cross section for each position along the sample axis, as was patented (Hyde, 1973). Since that possibility is technically difficult, the cross-sectional values reported in the early literature can be considered averages over optimum values along the sample axis. In all previous aqueous sample-cell designs, the cross section was sub-optimum along the sample, being too small at the ends and too large at the middle. Only the integral over the sample was optimum. A price was paid in sensitivity, which no longer needs to be paid when using a uniform field mode, since the cross section is optimum at every point along the sample axis. The present paper characterizes this observation in a quantitative manner.

In conventional geometries, it would be possible to vary the length of the aqueous sample by changing the diameter D to length L ratio for the cylindrical TE_{011} mode or the height Z to length Y ratio for the rectangular TE_{102} mode. We are not aware of an investigation of the effect of D/L or Z/Y on aqueous sample cell design and performance, and that would be a useful exercise. The question of optimum sample length is more compelling for the uniform field modes, since the length can be varied freely without shifting the resonant frequency. This is a further purpose of the present study.

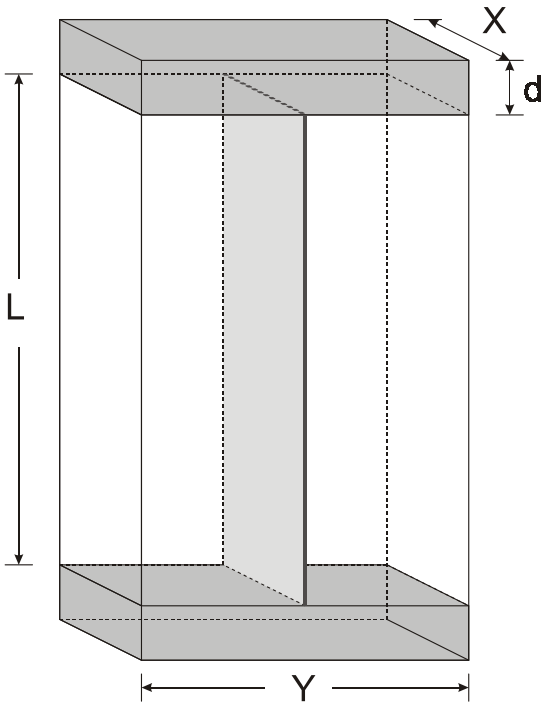

Fig. 1. Rectangular TE_{U02} mode, see Mett, Froncisz and Hyde (2001). Here d is the dielectric thickness, X and L are free parameters and Y is the free space wavelength. The cavity is analogous to the TE102 mode. The aqueous sample lying in the nodal plane of zero electric field is illustrated.

THEORY

Our analytic solution to the rectangular TE_{U02} uniform field mode in the presence of an aqueous flat cell is an extension of the work presented by Mett *et al.* (2001). First, we recast the theory of transverse material discontinuity given in Sec. III A of this paper in the rectangular geometry shown in Fig. 1. The fields (and wave functions) are uniform in the dimension x. Using a sample thickness $2a$, the transverse wave functions are,

$$\psi_2 = H_1 \cos\gamma_2 y, \quad 0 < y < a \tag{1}$$

$$\psi_1 = A\cos\gamma_1 y + B\sin\gamma_1 y, \quad a < y < Y/2 \tag{2}$$

Table 1. X-Band Aqueous Sample *Q* Ratios[a] (Wilmshurst, 1967).

Geometry	Sample type	Q ration
Rectangular TE_{102} with flat cell	saturable	1/3
	non-saturable	2/3
Cylindrical TE_{011} with capillary	saturable	indeterminate[b]
	non-saturable	1/2

[a]The sample should be such that the matched loaded *Q* is reduced to the tabulated function of the matched loaded Q of the empty cavity; [b]The radius should be as large as possible.

where H_1 represents the magnitude of the RF magnetic field at the center of the sample (the origin), and the transverse wave numbers are given by γ_1 and γ_2. Further, in this geometry, the unit normal to the material boundary $n = y$, a unit vector in the y direction, and the transverse gradient $\nabla_t = \hat{y}\partial/\partial y$. Then in combining continuity of axial RF magnetic field H_z across the dielectric with the boundary condition at the wall,

$$\partial\psi_1\partial y\big|_{y=Y/2} = 0 \tag{3}$$

we find,

$$A = (H_1 \cos\gamma_2 a)/\left[\cos\gamma_1 a + \sin\gamma_1 a \tan\gamma_1 Y/2\right], \tag{4}$$

$$B = (H_1 \cos\gamma_2 a)/\left[\sin\gamma_1 a + \cos\gamma_1 a \cot\gamma_1 Y/2\right]. \tag{5}$$

In combining these with the continuity of tangential electric field across the dielectric boundary, we obtain, after some algebra, the equation,

$$\gamma_2 \cot\gamma_2 a = -\gamma_1 \cot[\gamma_1 (Y/2 - a)] \tag{6}$$

Equations (4) - (6) are the rectangular analogs to Eqs. (81) - (83) of Mett *et al.* (2001). Equation (6) is also the same as Eq. (12) of Stoodley (1963), except that here the context is that of the TE_{U02} uniform field mode instead of the standard TE_{102} mode and we permit the transverse wave numbers to be complex rather than real.

Next, the theory of coupled transverse and axial material discontinuities outlined in Sec. III C of Mett *et al.* (2001) is applied. We permit the transverse and axial wave numbers of the purely transverse and radial problems to assume their respective roles in the coupled transverse and radial problem and ignore the fields in the relatively small region $0 < y < a$, $L/2 < z < L/2 + d$. This is done by solving the system of five equations and five unknowns given by Eq. (6) above, combined with Eqs. (85) and (12) of Mett *et al.* (2001):

$$\begin{aligned}\omega^2/c^2 = \gamma_1^2 + k_1^2 &= (\gamma_1^2 + k_2^2)/\varepsilon_{rd} \\ &= (\gamma_2^2 + k_1^2)/\varepsilon_{rs},\end{aligned} \tag{7}$$

$$k_1 \tan k_1 L/2 = k_2 \cot k_2 d. \tag{8}$$

Here, ω designates the radian frequency, c the speed of light in vacuum, k the axial wave number, and ε_{rd} and ε_{rs} the relative dielectric constants of the end dielectrics and sample, respectively. Subscripts 1 and 2 designate the regions without or with dielectric, respectively. With dielectric losses, the dielectric constants are complex and all the five unknowns ω, γ_1, γ_2, k_1, k_2 are generally complex. This system of equations was solved numerically using a Mathematica 4.1 root solver. The solution was found by starting from the exact uniform field mode solution $k_1 = 0$ for no sample. The thickness of the end dielectrics and the Y dimension of the cavity in this case are given by

$$d = \tfrac{1}{4} c\,\mathrm{Re}[(\varepsilon_{rd} - 1)^{-1/2}]/f_0 \tag{9}$$

$$Y = c/f_0, \tag{10}$$

where the subscript 0 is used on the frequency to denote the desired real operating frequency of the resonator and distinguish it from the numerical solution $\omega = 2\pi f$.

In the coupled problem, the transverse wave functions given by Eqs. (1) and (2) above are generalized, respectively, as

$$\psi_2 \to \psi_{21}, \quad 0 < y < a, \quad -L/2 < z < L/2, \tag{11}$$

$$\psi_2 \to \psi_{11}, \quad a < y < Y/2, \quad -L/2 < z < L/2, \tag{12}$$

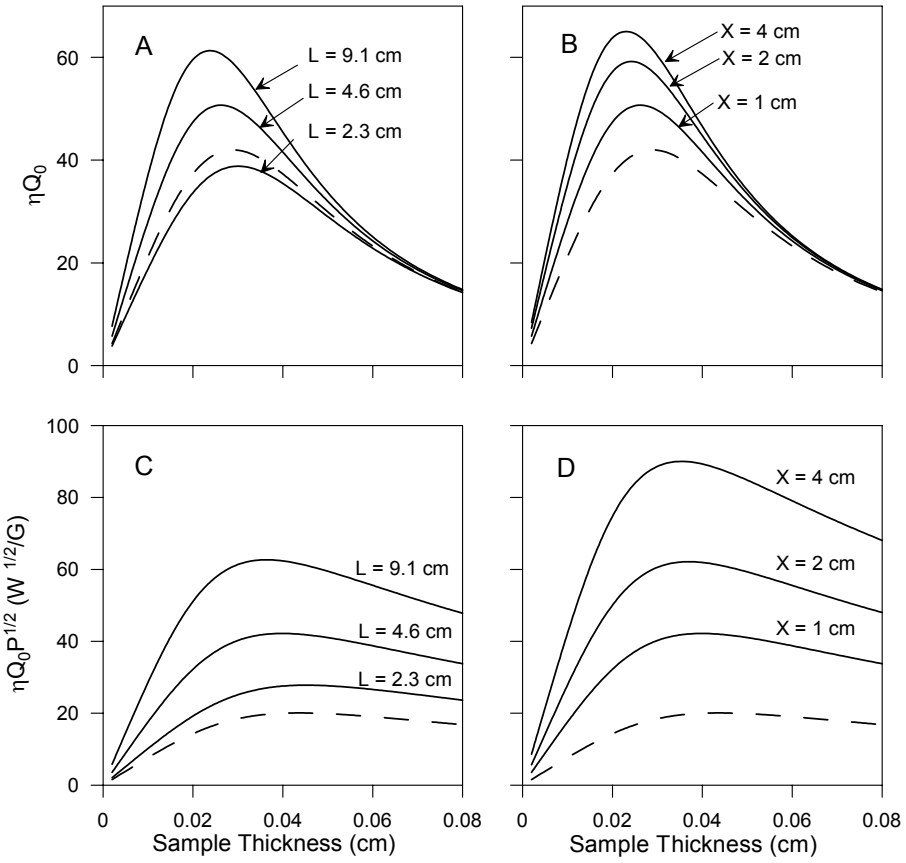

Fig. 2. Summary of calculations of signal intensities as a function of aqueous sample thickness. The dashed curves are for the standard rectangular TE_{102} cavity for reference. Upper plots (A, B) are for unsaturable samples and lower plots (C, D) for saturable. Left two plots (A, C) are for the free parameter X set to the inner diameter of X-band waveguide (0.400 inches or 1.016 cm). The length L is varied. Right two plots (B, D) are for the length L set to 4.6 cm. The free parameter X is varied.

where the first subscript corresponds to the transverse and the second subscript the axial. We apply continuity of axial RF magnetic field across the end dielectrics and obtain,

$$\psi_{12} = \psi_{21} \cos(k_1 L/2)/\sin k_2 d\,. \tag{13}$$

The fields of the resulting TE_{U02} (nearly) uniform field mode are found by substituting Eqs. (1), (2), and (11) - (13) above into Eqs. (61), (62) and (64) - (67) of Mett *et al.* (2001). In the region $0 < y < a$ and $-L/2 < z < L/2$,

$$H_z = H_1 \cos\gamma_2 y \cos k_1 z, \tag{14}$$

$$\mathbf{H}_t = (H_1 k_1/\gamma_2)\sin\gamma_2 y \sin k_1 z\ \hat{y}, \tag{15}$$

$$\mathbf{E}_t = (-i\omega\mu_0\, H_1/\gamma_2)\sin\gamma_2 y \cos k_1 z\ \hat{x}\,, \tag{16}$$

in the region $a < y < Y/2$ and $-L/2 < z < L/2$,

$$H_z = (A\cos\gamma_1 y + B\sin\gamma_1 y)\cos k_1 z, \tag{17}$$

$$\mathbf{H}_t = (k_1/\gamma_1)(A\sin\gamma_1 y - B\cos\gamma_1 y)\sin k_1 z\ \hat{y}, \tag{18}$$

$$\mathbf{E}_t = (-i\omega\mu_0/\gamma_1)(A\sin\gamma_1 y - B\cos\gamma_1 y)\cos k_1 z\ \hat{x}\,, \tag{19}$$

and in the region $a < y < Y/2$ and $L/2 < z < L/2 + d$,

$$H_z = \left[\cos(k_1 L/2)/\sin k_2 d\right](A\cos\gamma_1 y + B\sin\gamma_1 y) \sin\left[k_2(L/2 + d - z)\right], \tag{20}$$

$$\mathbf{H}_t = (k_2/\gamma_1)\left[\cos(k_1 L/2)/\sin k_2 d\right](A\sin\gamma_1 y - B\cos\gamma_1 y)\cos\left[k_2(L/2 + d - z)\right]\hat{y}, \tag{21}$$

$$\mathbf{E}_t = (-i\omega\mu_0/\gamma_1)\left[\cos(k_1 L/2)/\sin k_2 d\right](A\sin\gamma_1 y - B\cos\gamma_1 y)\sin\left[k_2(L/2 + d - z)\right]\hat{x}. \tag{22}$$

In these expressions, μ_0 represents the magnetic permeability of free space and $\hat{x}$ represents a unit vector in the x-direction.

In consideration of energy balance for time harmonic fields in the presence of lossy dielectrics, e.g. Jackson (1975) Sec. 6.10, expressions were obtained for the stored energy W and dissipated

power P_l in the cavity in terms of the preceding expressions for the fields,

$$W = W_v + W_d + W_s, \tag{23}$$

where

$$W_v = \tfrac{1}{2}\varepsilon_0 \int_{\text{vacuum region}} \mathbf{E}\cdot\mathbf{E}^* dV, \tag{24}$$

$$W_d = \tfrac{1}{2}\varepsilon_0 \,\mathrm{Re}(\varepsilon_{rd}) \int_{\text{end dielectrics}} \mathbf{E}\cdot\mathbf{E}^* dV, \tag{25}$$

$$W_s = \tfrac{1}{2}\varepsilon_0 \,\mathrm{Re}(\varepsilon_{rd}) \int_{\text{sample}} \mathbf{E}\cdot\mathbf{E}^* dV, \tag{26}$$

and

$$P_l = P_w + P_d + P_s, \tag{27}$$

where

$$P_w = (2\sigma\delta)^{-1} \int_{\text{walls}} (\hat{n}\times\mathbf{H})\cdot(\hat{n}\times\mathbf{H})^* dS, \tag{28}$$

$$P_d = \mathrm{Re}(\omega)\varepsilon_0 \,\mathrm{Im}(\varepsilon_{rd}) \int_{\text{end dielectrics}} \mathbf{E}\cdot\mathbf{E}^* dV, \tag{29}$$

$$P_s = \mathrm{Re}(\omega)\varepsilon_0 \,\mathrm{Im}(\varepsilon_{rs}) \int_{\text{sample}} \mathbf{E}\cdot\mathbf{E}^* dV. \tag{30}$$

In Eq. (28), σ is the wall conductivity and the skin depth $\delta = (\pi f_0 \mu_0 \sigma)^{-1/2}$. Further, integrals representing the unsaturable and saturable signal strengths were formed,

$$S_u = (P_{in}^{1/2}/P_l) \int_{\text{sample}} \mathbf{H}\cdot\mathbf{H}^* dV, \tag{31}$$

$$S_s = P_l^{1/2} \int_{\text{sample}} \mathbf{H}\cdot\mathbf{H}^* dV, \tag{32}$$

It is noted that $\eta Q_0 = \pi\, f_0\, \mu_0\, S_u$ with $\mathrm{P}_{in}{}^{1/2} = 1$, where η is the filling factor and Q_0 is the unloaded Q. The loaded Q when the cavity is matched is two times smaller. In the unsaturable case, the input power is set to some value, say 1W, and the reference magnetic field strength H_1 cancels out of the expression. In the saturable case, $\mu_0 H_1$ is set to some value, say 1G, and the input power (which is equal to P_l) is adjusted to achieve this.

The integrals were carried out analytically with the use of complex trigonometric identities such as $\sin\theta(\sin\theta)^* = \tfrac{1}{2}\cos[2\mathrm{Im}(\theta)] - \tfrac{1}{2}\cos[2\mathrm{Re}(\theta)]$. The results are too lengthy to show in this paper. The Q_0 value is given by

$$Q_0 = \mathrm{Re}(\omega) W / P_l. \tag{33}$$

Note that Q_0 does not account for energies or losses in the thin neglected region $0 < y < a$, $L/2 < z < L/2 + d$, consistent with the field expressions.

For purposes of comparison, the full wave calculations of all the preceding quantities were also found for the standard TE_{102} mode. In this case, $d \to 0$, $k_1 = \pi/L$, k_2 becomes arbitrary, and $R = (4f_0^2/c^2 - 1/L^2)^{-1/2}$. The system is reduced to three unknowns, ω, γ_1, and γ_2, and three equations given by Eq. (6) and the pair

$$\omega^2/c^2 = \gamma_1^2 + k_1^2 = \left(\gamma_2^2 + k_1^2\right)/\varepsilon_{rs} \tag{34}$$

RESULTS

This system was solved simultaneously in the same manner as for the TE_{U02} mode. With these values of frequency and wave number, the appropriate limiting expressions for the integrals were

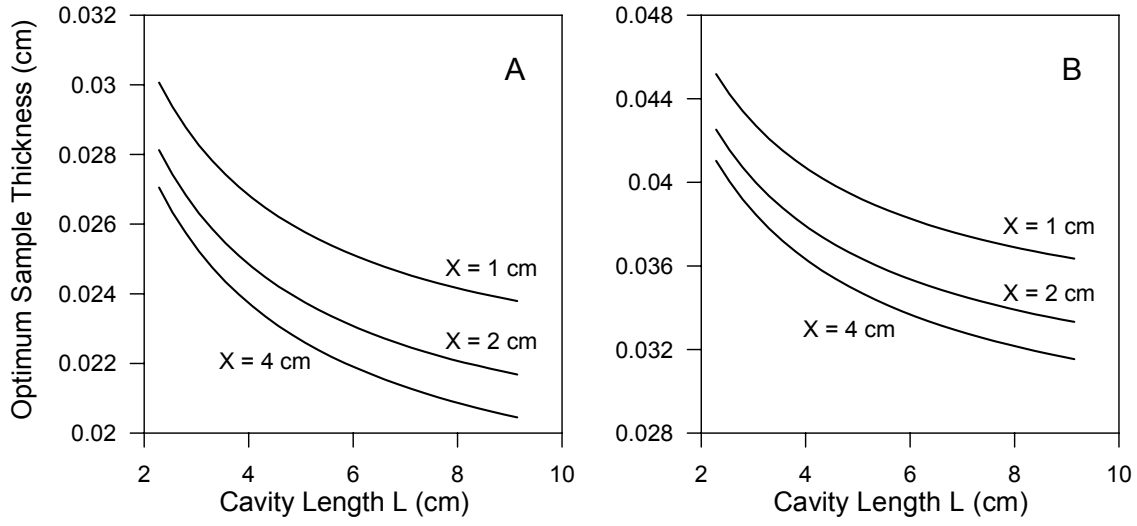

Fig. 3. Optimum aqueous sample thickness for non-saturable samples (A) and saturable samples (B) as a function of free parameters X and L.

evaluated numerically. All systems of equations were solved and expressions evaluated using Mathematica 4.1 (Wolfram Research, Inc. 1999, Champaign, IL).

Calculated values of Q_0(102) from our integral expressions were compared under the limit of zero sample thickness to values from the standard formulae given by Montgomery (1948) and agreement was found. Calculated values of Q_0(U02) in the limit of zero sample thickness resulting from end dielectric losses together with wall losses were compared to those predicted by Ansoft High Frequency Structure Simulator, version 8.0.25 (Ansoft Corp., Pittsburgh, PA), and agreement was found. All calculations were carried out on a dual processor Compaq W8000 workstation, with two Intel Xeon 1.7GHz Pentium processors. The operating frequency f_0 was set at 9.500 GHz. The dielectric constants were taken from Von Hippel (1954): the dielectric ends were taken as quartz, $\varepsilon_{rd} = 3.78(1 + 10^{-4}i)$ and the sample was taken as water at 25°C, $\varepsilon_{rs} = 55(1 + 0.54i)$. The conductivity of the walls was that of copper, $\sigma = 5.80\ 10^7/(\Omega\text{m})$.

Figure 2 summarizes the major results of this paper. Following the general theory of sensitivity by Feher (1956), the EPR signal for a reflection activity employing a linear microwave detector (i.e. sensitive to the microwave voltage rather than the microwave power) can be written

$$S \propto \chi \eta Q_0 P_{in}^{1/2}, \tag{35}$$

where χ is the RF susceptibility. If the sample cannot be saturated with the available microwave power, P_{in} and χ are constant and a calculation of the ηQ_0 product permits theoretical comparison. This calculation has been done in Figs. 2A and 2B for varying geometries. Examples of samples of this class are Mn^{2+} or Cu^{2+}.

Referring to Eq. (35), consider the case where the sample can be saturated and the saturation parameter in the denominator of the term χ becomes important. To compare aqueous cell geometries for this class of samples, one imagines $P_{in}^{1/2}$ to be readjusted in all comparisons such that the RF field at the sample remains constant. Thus from an engineering perspective, for non-saturable samples, P_{in} is held constant and for saturable samples, H_1 is held constant. Aqueous sample cell calculations are presented in Figs. 2C and 2D. Examples of such samples are spin labels and free radicals in aqueous solvent.

The length of the sample cell in the standard TE_{102} rectangular cavity is 2.3 cm. The performance of the uniform field and standard cavities are similar for non-saturable samples (Fig. 2A) when the sample length L and the free parameter dimension X correspond to the dimensions of X-band waveguide. There is a benefit of 30% for the uniform field mode for saturable samples, Fig. 2C. Doubling of the free parameter L from 2.3 to 4.6 cm yields additional benefit. For the saturable sample class, Fig. 2C, the uniform field mode has about twice as much sample ($L = 4.6$ cm versus 2.3 cm) and yields about twice the signal. Probably a choice of $L = 9.1$ cm (four times the normal broad face dimension of X-band waveguide) will result in an awkwardly long sample that places demands on the magnet homogeneity. This case has been included in the calculation to bracket our general conclusion that a choice of $L = 4.6$ cm seems to be about right.

The free parameter X is also of interest. Resonators oscillating in the TM_{110} mode, which is essentially similar to the TE_{102} mode, with the X dimension doubled were introduced commercially by one of us (J. S. Hyde) and are commercially available from Bruker Analytik (Karlsruhe, Germany). As is apparent from Figs. 2B and 2D, which were for $L = 4.6$ cm, additional benefit is obtained if X is increased, as was found previously for the TM_{110} cavity. However, in our judgment, a 4 cm wide flat cell seems unwieldy, and a choice of 2 cm seems reasonable.

Saturable samples, particularly spin labels, are much more commonly used in EPR spectroscopy than in non-saturable samples. The calculations of Fig. 2 lead to the conclusion that $L = 4.6$, $X = 2$ cm is a practical geometry that requires four times more sample than a conventional sample geometry in a rectangular TE_{102} rectangular cavity, and yields three times higher signal intensity.

It is noted from Fig. 2 that the optimum flat cell thickness is not the same for saturable and non-saturable samples. This point is also emphasized in Fig. 3. It is apparent also from an inspection of Figs. 2C and 2D that the falloff in sensitivity at larger sample thicknesses is very gradual. Curves such as seen in Figs. 2C and 2D also do not appear in the standard citations, and may be new. The gradual falloff may be important for EPR in tissue samples where the sample thickness is difficult to control.

Qualitatively, the sensitivity benefits of the uniform field mode arise from the following factors: (i) the dimension Y is 1.5 times smaller than in the standard cavity, improving the filling factor; (ii) the flat cell thickness is optimum at every point along L; (iii) the area over which the electric field is zero, the XL product, is unrestricted. The pri-

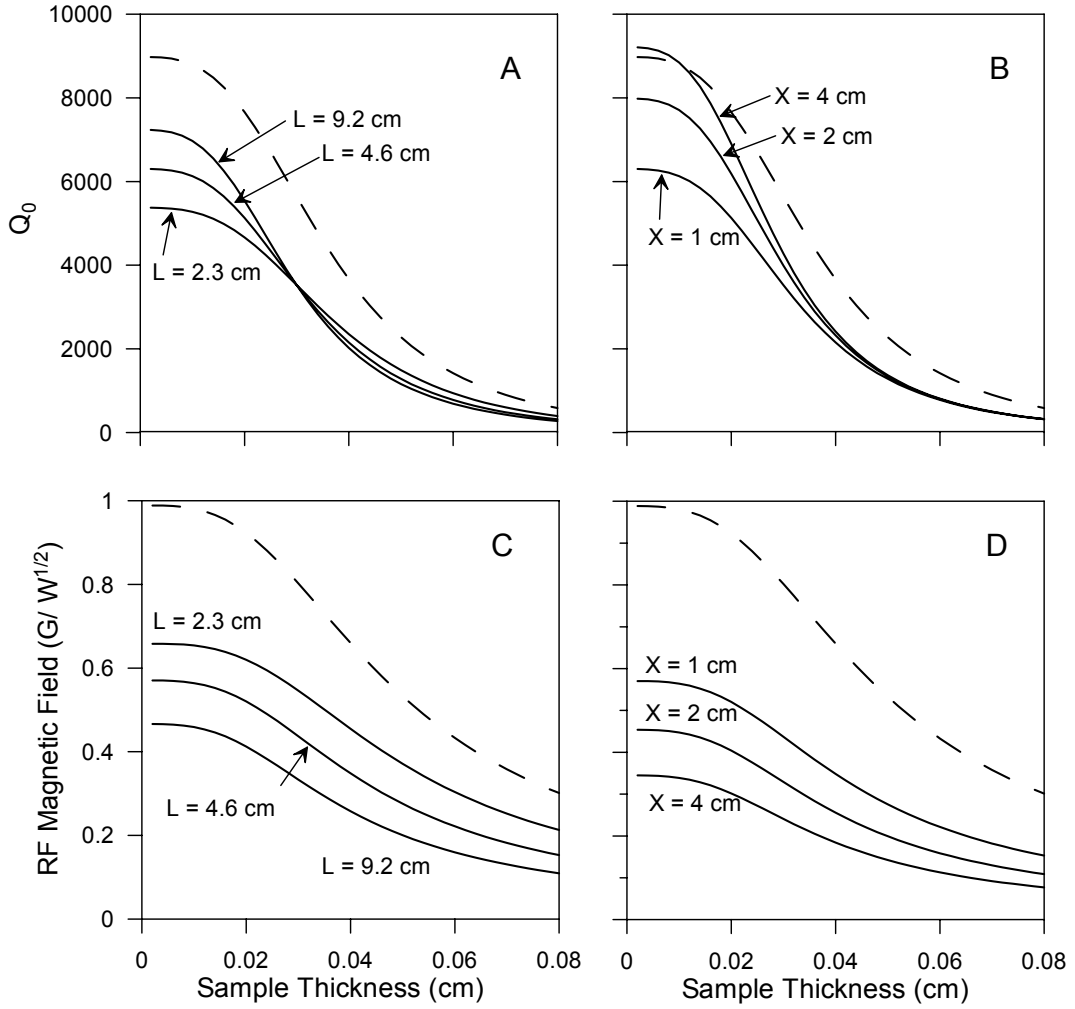

Fig. 4. Q_0 values A, B and rotating frame RF magnetic field values for a matched resonator C, D as a function of sample thickness. A, C are for constant X = 1 cm as a function of L, and B, D are for constant L = 4.6 cm as a function of X. The dashed curve is for the standard TE_{102} rectangular cavity.

mary disadvantage is loss of Q because of loss in the dielectric at the ends of the resonator.

Figure 2 demonstrates that there is a substantial advantage in using the TE_{U02} uniform field mode for aqueous samples with respect to signal-to-noise ratio in addition to the advantage with respect to the standard resonator that the RF magnetic field is uniform over the sample. Non-linear experiments including CW saturation, saturation transfer, electron-electron double resonance (ELDOR), pulse ELDOR, saturation recovery, free induction decay and spin echo will all benefit from a uniform field over the sample, resulting in data of higher quality. Contamination of data from sample segments that lie in differing regions of the sinusoidally varying RF field intensity will no longer be a confounding factor.

Figure 3 extracts data from the analysis of Fig. 2 concerning optimum sample thickness for non-saturable (3A) and saturable (3B) samples. In addition, optimum sample thicknesses have been calculated for the standard TE_{102} cavity – saturable, 0.44 mm, non-saturable, 0.29 mm. Variation of sample thickness is not convenient for quartz sample cells. Hyde (1972) presented a technique for machining sample cells of precise thickness from plastic, which may be useful to optimize the signal intensity.

Figures 4A and 4B show Q_0 values as a function of the experimental parameters L, X and sample thickness $2a$. The dashed lines are for the standard TE_{102} rectangular cavity. It is noted that the ideal Q_0 value for this cavity, about 9000, is above the practical value of about 7500. This figure may be useful to the EPR instrument designer in the following circumstances:

(i) dominant source phase noise, (ii) dead time problems in pulse EPR, (iii) ELDOR or other experiments where more than one microwave frequency is incident on the sample, (iv) resonator

sample geometries that are prone to microphonics. In these circumstances, it may be desirable to trade signal intensity for lower *Q*-value.

Similarly, Figs. 4C and 4D show RF magnetic field values as a function of the experimental parameters. This figure provides information to the EPR spectroscopist concerning whether or not the sample in which he is interested fits the "non-saturable" or the "saturable" condition. It can also be used to set initial conditions for comparison of uniform field resonators with the conventional TE_{102} resonator.

Table 1 shows that the optimum flat cell for a saturable sample in the standard TE_{102} rectangular cavity should lower the *Q* value to 1/3 of the value when empty. The factor changes to 2/3 for non-saturable samples. These ratios have been recalculated for the uniform field TE_{U02} mode as a function of *L* (see Fig. 1) with *X* set at the narrow dimension of X-band waveguide (0.400 inches or 1.016 cm). For saturable samples, the factor varies from 0.347 when *L* is relatively short to 0.344 for *L* relatively long. For non-saturable samples, a value of 0.654 was obtained for short *L* and 0.659 for long *L*. The factors were also recalculated for the standard TE_{102} cavity: 0.345, 0.655. It is concluded for practical purposes that Wilmshurst's values of 1/3, 2/3 remain valid for both uniform field and conventional resonators.

CONCLUSIONS

Modern computation capabilities permit analyses not previously practical, including finite element solutions of Maxwell's equations and numerical solutions of systems of equations. These capabilities have led to the development of a new class of microwave cavities for use in EPR spectroscopy, namely, uniform field modes. In the present study, they have enabled a theoretical investigation for aqueous sample-cell design for the rectangular TE_{U02} uniform field mode. Based on this analysis, a practical TE_{U02} mode for use with aqueous samples is currently under construction in the authors' laboratory.

Acknowledgment

This work was supported by grants GM-27665 and RR-01008 from the National Institutes of Health. Professor J.B. Feix, Medical College of Wisconsin, asked a question during the workshop concerning the suitability of uniform field resonators for aqueous samples. We thank him for the question.

Abbreviations

EPR, electron paramagnetic resonance; RF, radio frequency; TE, transverse electric.

REFERENCES

Alger R. S. (1968). *Electron paramagnetic resonance; Techniques and applications*. Interscience: New York.

Feher G. (1956). Sensitivity Considerations in microwave paramagnetic resonance absorption techniques. *Bell System Technical Journal*, **36**, 449.

Hirshon J. M. & Fraenkel G. K. (1955). Recording high-sensitivity paramagnetic resonance spectrometer. *Rev. Sci. Instrum.*, **26**, 34.

Hyde J. S. (1972). A New Principle for Aqueous Sample Cells for EPR. *Rev. Sci. Instrum.*, **43**, 629-631.

Hyde J. S. (1973). Cavity resonator structure for an EPR spectrometer employing dielectric material for improving RF electric and magnetic field uniformity along the sample, U.S. Patent 3,757,204.

Hyde J. S. (1965). *Signal amplitudes in electron paramagnetic resonance*. Varian Associates Technical Information Bulletin, Palo Alto: CA.

Jackson J. D. (1975). *Classical electrodynamics.* 2nd ed., Wiley: New York.

Mett R. R., Froncisz W. & Hyde J. S. (2001). Axially uniform resonant cavity modes for potential use in electron paramagnetic resonance spectroscopy. *Rev. Sci. Instrum.*, **72**, 4188.

Montgomery C. G. (1948). *Techniques of microwave measurements.* Vol. 11 Radiation Laboratory Series, McGraw-Hill: New York.

Poole C. P. Jr. (1983). *Electron spin resonance.* Wiley: New York.

Stoodley L. G. (1963). The sensitivity of microwave electron spin resonance spectrometers for use with aqueous solutions. *J. Electron. Control*, **14**, 531.

Von Hippel A. (1954). *Dielectric materials and applications*, Artech House: Boston.

Wilmshurst T. H. (1967). *Electron spin resonance spectrometers*, Adam Hilger: London.